

Crystal structure and optical spectra of MnAs with a NiAs-type hexagonal structure

H. ALGARNI^{a,b}, A. GUEDDIM^{c,*}, N. BOUARISSA^d, O. A. AL-HAGAN^a, T. F. ALHUWAYMEL^e, M. AJMAL KHAN^a

^aDepartment of Physics, Faculty of Science, King Khalid University, P. O. Box 9004, Abha 61413, Saudi Arabia

^bResearch Center for Advanced Materials Science (RCAMS), King Khalid University, P. O. Box 9004, Abha 61413, Saudi Arabia

^cMaterials Science and Informatics Laboratory, Faculty of Science, University of Djelfa, 17000, Djelfa, Algeria

^dLaboratory of Materials Physics and Its Applications, University of M'sila, 28000 M'sila, Algeria

^eNational Centre for Nanotechnology, King Abdulaziz City for Science and Technology (KACST), P. O. Box 6086, Riyadh 11442, Saudi Arabia

The crystal structure and optical spectra of MnAs with a NiAs-type hexagonal structure are investigated using spin-polarized full-potential calculations in the framework of the density functional theory within Wu-Cohen and Tran-Blaha-modified Becke-Johnson generalized gradient approximation approaches. Features such as lattice parameters, bulk modulus and its first-pressure derivative are presented. The evolution of the optical spectra as a function of the photon energy for both spin up and spin down channels is examined and discussed. The effect of spin channel on optical spectra is found to be significant. This may provide advantage of the spin degree of freedom making thus the material of interest as a potential candidate for use in fabrication of new functional spintronics materials.

(Received June 20, 2020; accepted February 15, 2021)

Keywords: Crystal structure, Optical spectra, MnAs; NiAs-structure, Spintronics

1. Introduction

The interest in magnetic materials is driven in part by the desire to use the spin degree of freedom in electronics. This has quickly expanded the field of spintronics and exploited metal based devices making thus a revolution in magnetic sensors [1-5]. In this respect, MnAs is a suitable material for spin-electronic and magneto-optic applications [6-12]. The material of interest presents also many advantages over transition metals as regards the metallic component in metal/semiconductor structures [7]. MnAs crystallizes in three different structures, namely the NiAs-type hexagonal structure as natural, the MnP-type structure in an experimental mode, and the hypothetical zinc-blende mode that has not yet been seen in nature [12,13].

The chemical and physical properties of materials can be explained by the structure and the arrangements of atoms. In fact, the structural properties can give a useful information on the rigidity, strength and toughness of the material under investigation [14-17]. On the other hand, the optical properties of materials have provided rich information on such diverse aspects of their physical properties [18,19]. These properties depend on the interaction of electromagnetic radiation with matter which is linked to the wavelength and frequency of the radiation and material property such as dielectric constants, refractive index, reflectivity, optical absorption and so on [20,21].

The present investigation reports on the crystal structure and optical spectra of MnAs material with a NiAs-type hexagonal structure. The computations are performed using spin-polarized full-potential linearized augmented-plane wave (FP-LAPW) method which employs the density functional theory (DFT). The exchange-correlation potential has been described using the Wu-Cohen generalized gradient approximation (WC-GGA) for studying the crystal structure and Tran-Blaha modified Becke-Johnson GGA (TB-mBJ-GGA) approach for investigating the optical properties. More details about the computations are given in section 2 of this paper.

2. Computational framework

First-principles band structure and total-energy calculations have been carried out within the framework of the DFT [22,23]. The WC-GGA [24] and TB-mBJ-GGA [25] approaches have been used in order to treat the exchange-correlation potential. The spin-polarized FP-LAPW method as implemented in the WIEN2K code [26] is used and applied to a two-atoms unit cell. In the FP-LAPW method, the space is divided into two regions: a non-overlapping muffin tin (MT) spheres region where the spheres are centered at the atomic sites and an interstitial region where the basis set consists of plane waves.

The magnitude of the largest k vector in the plane wave expansion (k_{\max}) is taken to be $7.0/R_{\text{MT}}$, where R_{MT} is the smallest of all atomic sphere radii. The adopted

muffin-tin radii are 2.0 atomic units for Mn atom and 2.1 atomic units for As atom. The separation energy between the valence and the core states is -6.0 Ryd. A $10 \times 10 \times 10$ k-point grid has been adopted to sample the Brillouin zone using a procedure similar to that described in Refs. [27,28]. The total energy and eigenvalues are converged to 10^{-5} and 10^{-4} Ryd, respectively.

Fig. 1 displays the crystallographic cell of MnAs with NiAs-type crystal structure.

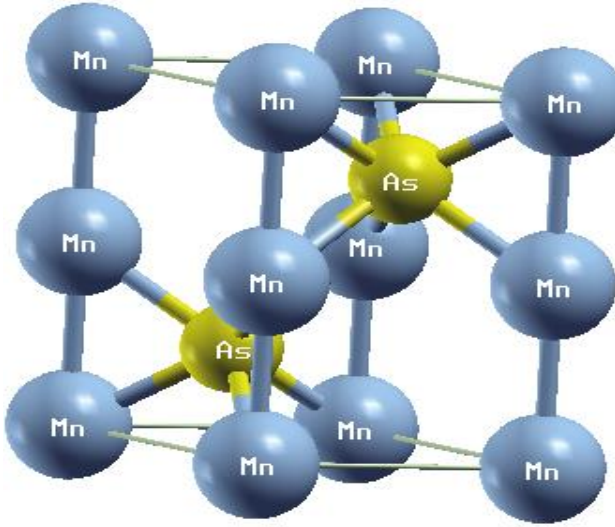


Fig. 1. Crystallographic cell of MnAs with NiAs-type crystal structure (color online)

3. Results and discussion

3.1. Crystal structure

The NiAs-type hexagonal structure has been considered which is the natural phase. Its space group is $p6_3/mmc$. In this structure, MnAs is a ferromagnetic metal [12]. The structural parameters are obtained using WC-GGA approach [24]. The equilibrium structural parameters such as the lattice constants a_0 and c_0 , the bulk modulus B_0 and its first-pressure derivative B_0' have been determined. This has been done by fitting the data that represent the variation of the total energy versus the volume to the Murnaghan's equation of state. The procedure is similar to that used previously in Refs. [29,30]. Our results yielded values of $a_0=3.586$ Å, $c_0=5.311$ Å, $B_0=99.038$ GPa and $B_0'=5.12$. The experimental lattice constants of MnAs with a NiAs-type hexagonal structure as reported in Refs. [9,12,31] are $a_0=3.722$ Å and $c_0=5.702$ Å. Our results show very good accord with those of experiment [9,12,31] in that the agreement between our obtained a_0 and that of experiment is within 3% and the deviation between our calculated c_0 and that of experiment is less than 7%. For the fact that there are no experimental or theoretical data regarding B_0 and B_0' for MnAs with NiAs-type hexagonal structure, to the best of our knowledge, our calculated B_0 and B_0' are predictions.

3.2. Optical spectra

The accurate knowledge of the refractive index (n) is very important for designing and fabricating devices [32-37]. In the present contribution, the refractive index spectra, $n(E)$, where E is the incident photon energy, have been computed for MnAs with NiAs-type structure for both spin up and spin down channels using TB-mBJ-GGA approach. Our results are plotted in Fig. 2. For a null photon energy, our calculation yielded values for static refractive index of $n=11.60$ and $n=17.46$ for spin up and spin down channels, respectively. We see that at low photon energies the values of n are more important than at high photon energies. This is true for both spin up and spin down channels. A similar qualitative behavior of $n(E)$ as a function of photon frequency (energy) has been reported by Khan and Bouarissa [38] for ZnS at different temperatures using molecular dynamics simulation. An appearance of peaks can be observed. These peaks are originated from the excitonic transitions. Generally, these peaks are more pronounced at the spectrum for spin up than at the spectrum for spin down. The tendency of the excitonic effects is to increase the oscillator strength at M_0 and M_1 points [39,40]. The main peak in $n(E)$ is related essentially to the 2D exciton transitions. The effect of varying the spin channel appears to be important on $n(E)$ of MnAs of interest.

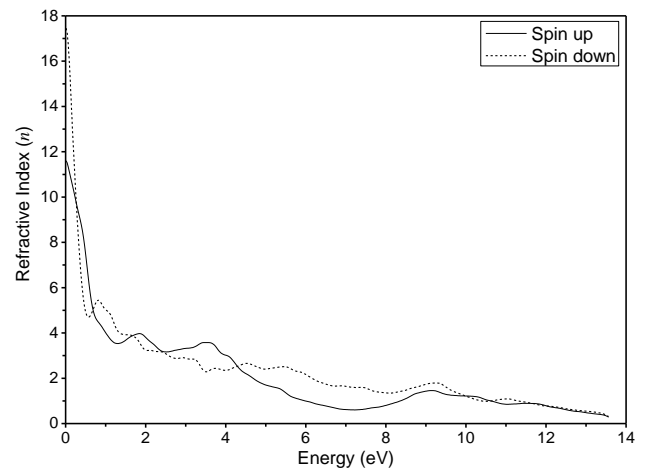


Fig. 2. Refractive index spectra for MnAs with NiAs-type crystal structure for spin up and spin down channels

The reflectivity (R) is an important measurable optical parameter. This parameter is generally derived from the complex dielectric function. In the present work, R is determined for MnAs material with a NiAs-type hexagonal structure for both spin up and spin down channels using TB-mBJ-GGA approach in the photon energy interval 0-14 eV. Our computed reflectivity spectra for MnAs are shown in Fig. 3. Note that the reflectivity spectrum for the material being considered here presents a series of minor peaks in both spin up and spin down channels. These peaks are derived from interband transitions. The width of these peaks is attributed to

phonon-phonon scattering that is responsible for the vibrations damping. A similar qualitative behavior of R as a function of photon energy has been reported for MnX compounds and transition metals [9,41]. This is attributed to the isoelectric and isostructural nature of these materials. On the other hand, our results resembles to the overall trend of the experimental reflectivity spectra measured by Bärner et al. [42] for MnAs in the range 0.3-14 eV in the NiAs structure at room temperature. When varying the spin channel, the reflectivity spectra of MnAs are affected. We observe that when going from spin up to spin down channel, the maximum of $R(E)$ at zero photon energy becomes larger and it is further shifted towards low photon energies. At higher photon energies it becomes less important than that of spin up. Further, it increases again and becomes more important than the spectrum of spin up.

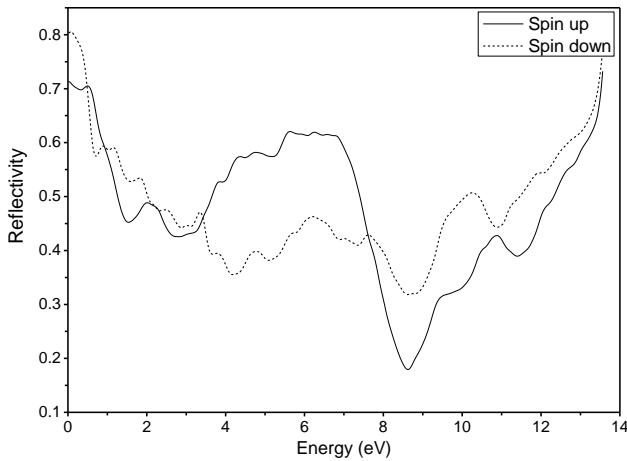


Fig. 3. Reflectivity spectra for MnAs with NiAs-type crystal structure for spin up and spin down channels

The optical absorption coefficient $\alpha(\omega)$ is a useful optical parameter that can be used for materials so as to check their utility in using them for the design and fabrication of devices. For that, $\alpha(\omega)$ has been computed in this work for MnAs with NiAs-type structure using TB-mBJ-GGA approach [25]. The incident photon energy is taken in the interval 0-14 eV. Both spin channels have been considered. Our results regarding α as a function of photon frequency (energy) are shown in Fig. 4. Note that the shape of the absorption coefficient spectrum for spin up channel resembles that of spin down channel but differs in details. The intensities for spin up channel appears to be higher than those for spin down channel in the photon energy interval 3.5-6 eV. However, the reverse can be noted in the interval from about 6 to around 13.5 eV. Hence, there is an anisotropic character of $\alpha(\omega)$ for spin up and spin down channels.

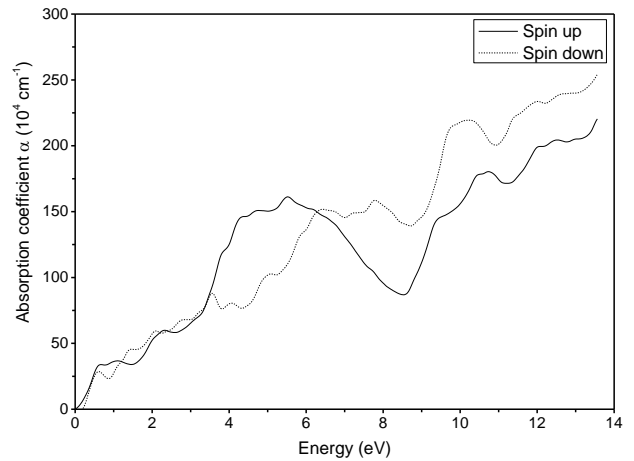


Fig. 4. Absorption coefficient spectra for MnAs with NiAs-type crystal structure for spin up and spin down channels.

The top value of $\alpha(\omega)$ for MnAs with NiAs-type hexagonal structure for spin up channel and occurs for the photon energy of about 5.5 eV. MnAs has an absorption band that is extended from 0 to 13.5 eV which depends on the energy of the absorbed light and the direction of the spin. Therefore, the material of interest offers a high optical absorption coefficient ($>10^4 \text{ cm}^{-1}$) with a large absorption band. Changing the direction of the spin affects generally the values of the optical absorption coefficient which becomes lower or higher depending on the incident photon energy interval.

For determining the electronic characteristics of materials, the knowledge of the optical conductivity can be a good probe [43,44]. In this respect, the optical conductivity of MnAs with NiAs-type structure has been calculated for both spin channels using TB-mBJ-GGA approach [25]. Our results are illustrated in Fig. 5. We observe that the optical conductivity depends strongly on the photon wavelength (energy). At low photon energy and for the spin up channel case more important optical conductivity can be observed compared with that at high photon energy. One can note a series of peaks from the spectrum of the optical conductivity. The top of the spectrum seems to be at a photon energy of about 4 eV. The situation seems to be different for the optical conductivity for the spin down channel case where the maximum of the spectrum occurs at a photon energy of about 9.5 eV and the optical conductivity appears to be less important at low photon energies than at high photon energies. Its spectrum exhibits series of peaks. The rate of absorption of incident photons by electrons seems to be strongly dependent on the photon wavelength (energy) and differs significantly when proceeding from spin up channel to spin down channel or vice versa.

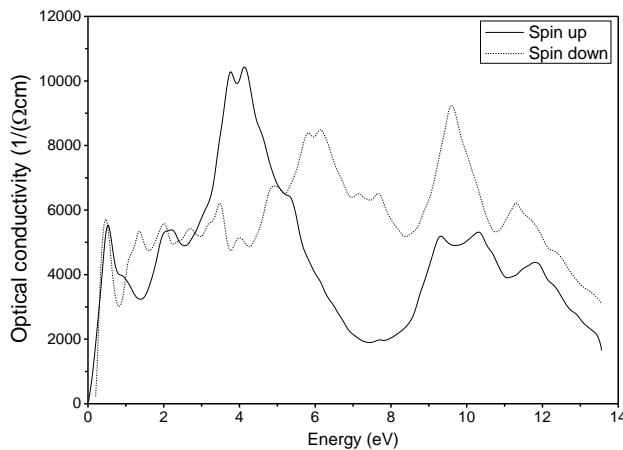


Fig. 5. Optical conductivity spectra for MnAs with NiAs-type crystal structure for spin up and spin down channels.

4. Conclusions

To conclude, the structural parameters and optical properties of MnAs material with the NiAs-type hexagonal structure were studied. The calculations were performed using the spin-polarized FP-LAPW method in the WC-GGA and TB-mBJ-GGA approaches. The obtained structural properties were found to agree well with those of experiment. The evolution of the optical spectra as a function of a photon energy in the interval 0-14 eV was examined and discussed for both spin up and spin down channels. The effect of varying the spin channel on the optical spectra was found to be significant. All optical features being studied here were also found to depend on the photon wavelength (energy). The information derived from the present study could be useful for the use of the material in question in the fabrication of new functional materials that could be used in spintronics application taking advantage of the spin degree of freedom.

Acknowledgements

The authors extend their appreciation to the Deanship of Scientific Research at King Khalid University, Abha, Saudi Arabia for funding this work through research groups program under grant number R.G.P. 2/24/40.

References

- [1] H. Ohno, *Science* **281**, 951 (1998).
- [2] S. A. Wolf, D. D. Awschalom, R. A. Buhrman, J. M. Daughton, S. Von Molnar, M. L. Roukes, A. Y. Chtchelkanova, D. M. Treger, *Science* **294**, 1488 (2001).
- [3] D. D. Awschalom, M. E. Flatté, *Nat. Phys.* **3**, 153 (2007).
- [4] I. Žutić, J. Fabian, S. Das Sarma, *Rev. Mod. Phys.* **76**, 323 (2004).
- [5] N. Bouarissa, S. Zerroug, S. A. Siddiqui, A. Hajry, *Superlatt. Microstruct.* **64**, 237 (2013).
- [6] R. de Paiva, J. L. A. Alves, R. A. Nogueira, J. R. Leite, L. M. R. Scolfaro, *J. Magn. Magn. Mater.* **288**, 384 (2005).
- [7] S. Sanvito, N. A. Hill, *Phys. Rev. B* **62**, 15553 (2000).
- [8] R. de Paiva, J. L. A. Alves, R. A. Nogueira, J. R. Leite, L. M. R. Scolfaro, *Brazilian J. Phys.* **34**, 568 (2004).
- [9] P. Ravinran, A. Delin, P. James, B. Johansson, J. M. Wills, R. Ahuja, O. Eriksson, *Phys. Rev. B* **59**, 15680 (1999).
- [10] A. Contineza, S. Picozzi, W. T. Geng, A. J. Freeman, *Phys. Rev. B* **64**, 085204 (2001).
- [11] K. Maki, T. Kaneko, H. Hiroyoshi, K. Kamigaki, *J. Magn. Magn. Mater.* **177-181**, 1361 (1998).
- [12] F. Moradiannejad, S. J. Hashemifar, H. Akbarzadeh, *J. Comput. Meth. Phys.* **1**, 1 (2013).
- [13] H. Ohno, *J. Magn. Magn. Mater.* **200**, 110 (1999).
- [14] F. Göde, *Optik* **197**, 163217 (2019).
- [15] S. Saib, N. Bouarissa, P. Rodríguez-Hernández, A. Muñoz, *Physica B* **403**, 4059 (2008).
- [16] R. Vinodkumar, J. Varghese, J. Varghese, N. V. Unnikrishnan, *Optik* **174**, 274 (2018).
- [17] N. Bouarissa, *Phys. Lett. A* **245**, 285 (1998).
- [18] V. Şenay, S. Özen, T. Aydoğmuş, *Optik* **191**, 15 (2019).
- [19] Z. Ma, C. Luo, C. Wang, J. Liu, *Optik* **188**, 104 (2019).
- [20] F. Mezrag, W. Kara Mohamed, N. Bouarissa, *Physica B* **405**, 2272 (2010).
- [21] N. Bouarissa, *Mater. Sci. Eng. B* **86**, 53 (2001).
- [22] P. Hohenberg, W. Kohn, *Phys. Rev.* **136**, B864 (1964).
- [23] W. Kohn, L. J. Sham, Self-consistent equations including exchange and correlation effects, *Phys. Rev.* **140**, A1133 (1965).
- [24] Z. Wu, R. E. Cohen, *Phys. Rev. B* **73**, 235116 (2006).
- [25] F. Tran, P. Blaha, *Phys. Rev. Lett.* **102**, 226401 (2009).
- [26] P. Blaha, K. Schwarz, G.K.H. Madsen, D. Kvasnicka, J. Luitz, 2014, WIEN2k code, An Augmented Plane Wave Plus Local Orbital's Program for Calculating Crystal Properties, Vienna University of Technology, Vienna.
- [27] H. J. Monkhorst, J. D. Pack, *Phys. Rev. B* **13**, 5188 (1976).
- [28] J. D. Pack, H. J. Monkhorst, *Phys. Rev. B* **16**, 1748 (1977).
- [29] S. Zerroug, F. Ali Sahraoui, N. Bouarissa, *Eur. Phys. J. B* **57**, 9 (2007).
- [30] S. Saib, N. Bouarissa, *Phys. Status Solidi B* **244**, 1063 (2007).
- [31] G. Schmidt, D. Ferrand, L. W. Molenkamp, A. T. Filip, B. J. Van Wees, *Phys. Rev. B* **62**, R4790 (2000).
- [32] S. Ozaki, S. Adachi, *J. Appl. Phys.* **75**, 7470 (1994).
- [33] N. Bouarissa, *Optik* **138**, 263 (2017).
- [34] K. Suzuki, S. Adachi, *J. Appl. Phys.* **83**, 1018 (1998).

- [35] N. Bouarissa, *Mater. Chem. Phys.* **72**, 387 (2001).
- [36] N. M. Ravindra, P. Ganapathy, J. Choi, *Infrared Phys. Technol.* **50**, 21 (2007).
- [37] M. Boucenna, N. Bouarissa, *Optik* **125**, 6611 (2014).
- [38] M. A. Khan, N. Bouarissa, *Optik* **124**, 5095 (2013).
- [39] P. Y. Yu, M. Cardona, *Fundamentals of Semiconductors, Physics and Materials Properties*, Springer-Verlag, Berlin, 1996.
- [40] A. Gueddim, S. Zerroug, N. Bouarissa, *J. Lumin.* **135**, 243 (2013).
- [41] H. Ehrenreich, *Optical Properties and Electronic Structure of Metals and Alloys*, edited by L. Abelés, Wiley, New York, 115 (1966).
- [42] K. Bärner, R. Braunstein, E. Chock, *Phys. Status Solidi* **80**, 451 (1977).
- [43] N. Bouarissa, A. Gueddim, S. A. Siddiqui, M. Boucenna, A. Al-Hajry, *Superlatt. Microstruct.* **72**, 319 (2014).
- [44] A. Bouarissa, A. Gueddim, N. Bouarissa, H. Maghraoui-Meherzi, *Optik* **208**, 164080 (2019).

* Corresponding author: ahmed_gueddim@yahoo.fr